Indirubin suppresses 4T1 murine breast cancer in vitro and in vivo by induction of ferroptosis and up-regulation of Ptgs2

Xiuping Kuang
Yunnan University of Traditional Chinese Medicine
Yingnan Jiang
Shenyang Pharmaceutical University
Jiwei Huang
Third Affiliated Hospital of Sun Yat-Sen University
Yongzhi Guo
Jinan University
weixi Li (liweixi1001@163.com)
Yunnan University of Traditional Chinese Medicine https://orcid.org/0000-0002-6614-9508

Research article

Keywords: Breast cancer, indirubin, ferroptosis, Ptgs2, GSK-3β

Posted Date: April 9th, 2021

DOI: https://doi.org/10.21203/rs.3.rs-390546/v1

Abstract

Background

Indirubin, isolated from *Indigo Naturals*, is reported to have the inhibitory activity of MCF-7 human breast cancer cells *in vitro*. However, studies on its anti-breast cancer activity *in vivo* and underlying mechanism are insufficient. We explored whether indirubin could trigger ferroptosis of breast cancer cells to exert anti-tumor activity.

Methods

Bioinformatical analysis was performed to detected the expression of *prostaglandin-endoperoxide synthase 2 (Ptgs2)* in breast cancer tissues *Ptgs2*-related prognosis for patients with breast cancer. Growth of 4T1 cells was assessed using wound healing assay and MTT assay. The levels of 4-HNE, GPX4, PTGS2 and GSK-3β proteins were detected by Western blot, and the mRNA of *Ptgs2* was tested by qPCR. The GSH and MDA were determined by commercial kits. Molecular docking was employed to study interaction between indirubin and GSK-3β. An 4T1 murine breast cancer was adopted to evaluate the *in vivo* antitumor activity of indirubin.

Results

Indirubin promoted ferroptosis of 4T1 breast cancer cells with deplete of GSH, increased MDA and 4-HNE level, as well as decreased GPX4 expression. Indirubin suppressed the growth of 4T1 breast tumor *in vivo*. Mechanism study showed indirubin up regulated *Ptgs2* expression by promoting phosphorylation (Ser 9) of GSK-3β.

Conclusions

Indirubin suppresses 4T1 murine breast cancer *in vitro* and *in vivo* by induction of ferroptosis and up-regulation of *Ptgs2*.

Background

Breast cancer is the most common cancer among women with increasing incidence year by year. Furthermore, it is also one of the leading causes of death among women with cancer worldwide [1–3]. Chemotherapy is one of the important methods for the treatment of breast cancer, but the drug resistance and side effects make it imperative to find new breast cancer treatment drugs [4–6].

Indigo Naturalis, the classical Chinese medicine, has been used in China for many centuries, and modern pharmacological studies have shown that it has anti-inflammatory, antiviral, antibacterial, anti-tumor and

anti-psoriatic activities [7–11]. In the study of the pharmacological active components of *Indigo Naturalis*, indirubin has received the most attention [12]. Indirubin, the major active component of *Indigo Naturalis*, have been widely known for its clinical use for treatment of chronic myelocytic leukemia (CML) [13, 14]. Recent studies have shown that indirubin can also be used to treat other types of cancer, like breast cancer [15–17]. However, the research on the mechanism of indirubin in the treatment of breast cancer is still insufficient.

Ferroptosis, a new type of cell death, is mediated by iron-dependent accumulation of lipid peroxidation. It was found that ferroptosis can be involved in the occurrence, progression and treatment of tumor. And emerging evidence indicates triggering ferroptosis of cancer cells is an important means for cancer therapy [18–21].

In this study, we aimed to explore whether indirubin could play an anti-breast cancer role by inducing the occurrence of ferroptosis. We analyzed the clinical data provided by NCBI database and found that breast cancer was related to the low level of *prostaglandin-endoperoxide synthase 2* (*Ptgs2)*, a molecular marker of ferroptosis. *In vivo* and *in vitro* studies suggested that indirubin could exert the anti-breast cancer effect by up-regulating PTGS2 and inducing ferroptosis.

Methods

Chemicals and reagents

Indirubin (wkq-01742, purity ≥ 97.0%, HPLC) and indigo (wkq-00174, purity ≥ 98.0%, HPLC) were purchased from Sichuan Weikeqi Biological Technology Co., Ltd (Chengdu, China). Primary antibodies to PTGS2 (GB11077-2) was purchased from Servicebio Co., Ltd (Wuhan, China). Primary antibodies, anti-GSK-3β (D5C5Z, #12456) and anti-phospho-GSK-3β (Ser 9, 5B3) (#9323), were purchased from Cell Signaling Technology (CST) (Boston, MA, USA). Primary antibodies to 4-HNE (ab46545) and GPX4 (ab125066) were purchased from Abcam (Cambridge, MA, USA). Adriamycin (A183027, purity ≥ 97.0%) was purchased from Shanghai Aladdin Bio-Chem Technology Co., LTD (Shanghai, China). Anti-glyceraldehyde 3-phosphate dehydrogenase (GAPDH) antibody (FD0063) was from Fude Biological Technology (Hangzhou, China). Other chemicals were purchased from standard commercial suppliers.

Bioinformatical analysis of breast cancer-related genes

The gene expression profile of GSE20713, GSE42568 and GSE 54002 in breast cancer and normal breast tissues were obtained from the free public database, NCBI-GEO database. Differentially expressed genes (DEGs) between breast cancer specimen and normal breast specimen were identified *via* GEO2R online tools with log FC < -2 and adjust *P* value < 0.05 [22]. Then, the raw data in TXT format were checked in Venn software online to detect the commonly DEGs among the three datasets. The prognostic relationships between selected genes and breast cancer were analyzed by Kaplan-Meier plotter and GEPIA online tools [23, 24].

Cell culture

4T1 mouse breast cancer cell was purchased from the Cell Bank of the China Academy of Sciences and cultured in DMEM medium (C11995500BT, Gibco, Carlsbad, CA, USA) supplemented with 10% fetal bovine serum (FBS) (ST40-39500, PAN-Seratech, Aidenbach, Germany) and 1% penicillin-streptomycin (C0222, Beyotime, Shanghai, China) at 37 °C under a humidified 5% CO_2 atmosphere.

Cell viability analysis

4T1 cells were seeded in a 96-well plate and cultured in DMEM supplemented with 10% FBS overnight. After 24 h of drug treatment, 3-(4,5-dimethyl-2-thiazolyl)-2,5-diphenyl-2-H-tetrazolium bromide (MTT) solution was added into each well and incubated at 37 °C for 4 h. The medium was removed and formazan crystals were later dissolved in dimethyl sulfoxide (DMSO). The absorbance was measured at 570 nm.

Wound healing assay

4T1 cells were seeded into 12-well plates and grown to a monolayer until 90% confluence. After removing the medium, the cell monolayer was scraped in a straight line with a sterile tip of 200 microliters. Next, the isolated cells were washed with phosphate buffer saline (PBS). The cells were treated with fresh medium containing 2% FBS with different drug concentrations for 48 h. Untreated cells served as the control. All the cells were photographed with a microscope before and after the drug treatment. Image J software was used to quantitatively calculate the wound area.

Animal experiment

BALB/c mice (6–8 weeks old, female) were purchased from Guangdong Medical Laboratory Animal Center (Guangzhou, China) with permission No. SCXK 2017 − 0174. Animal experiments were approved by the Animal Care and Use Committee of Jinan University and conducted in accordance with National Institute of Health's Guide for the Care and Use of Laboratory Animals (7th edition, United States). All mice were kept in a non-pathogenic animal chamber with a temperature of 23 ± 1 °C and a dark period of 12 h, and fed with standard laboratory diet and water. The animals were allowed to acclimatize for a week before the experiment. Mice received a subcutaneous injection with 4T1 cells (2×10^6 cells) into the right flank. When the tumor diameter reached about 5 mm, the mice were randomly divided into 5 groups. The mice were treated with saline, indigo (20 mg/kg), indirubin (low dose, 10 mg/kg; high dose, 20 mg/kg) and Adriamycin (1 mg/kg, clinically used in the treatment of breast cancer, as a positive control drug) every day (**Supplementary Table 1**). The tumor sizes were measured every 2 day using calipers, and the tumor volume was calculated by the following formula: volume (mm^3) = 0.5 × [length (mm)] × [width (mm)]^2. The tumor size at 21th day post-injection was used as the endpoint reading. Mice were sacrificed with diethyl ether anesthesia. The data were presented as the mean volume X ± S. E.

Histological analysis

Breast tumors were fixed with 4% paraformaldehyde for 48 h at room temperature. Then, they were dehydrated, transparent, paraffin-embedded and cut into 5 μm thick slices. Hematoxylin and eosin (H&E)

were used for staining of tumor tissues. The histological changes were observed and imaged at 40x magnification under an automatic scanning microscope (PreciPoint M8, Freising, Germany).

Western blotting

The cells and tumor tissues were lysed using RIPA (P0013C, Beyotime) lysis buffer containing 1 mM PMSF (P1005, Beyotime) on ice for 30 min. After centrifugation at 12,000 × *g* at 4 °C for 10 min, the supernatants were collected and total protein concentrations were determined using BCA protein assay kit (Pierce, Rockford, IL, USA). The protein samples were separated by 10% SDS-PAGE and then transferred to PVDF membranes (Millipore Corporation, Billerica, MA, USA). The membranes were blocked with 5% skim milk dissolved in TBST buffer at room temperature for 1 h and probed with the indicated primary antibodies at 4 °C overnight and then incubated with HRP-labeled secondary antibodies at room temperature for 2 h. Target proteins were detected using ECL Western Blotting Detection Reagent (20190120, Fude Biological Technology) and visualized by Tanon 5200 imaging system (Tanon, Shanghai, China). GAPDH is used as an internal control.

Reverse transcription and quantitative real-time PCR

Total RNA of cells was extracted using TRIzol reagent (Invitrogen, Carlsbad, CA, USA) according to manufacturer's instructions. RNA concentrations were determined by optical density measurement at 260 nm on a spectrophotometer (NanoDrop 2000, Thermo Scientific; Wilmington, DE, USA). cDNA was synthesized from the purified RNA by both random and oligo (dT) priming by a TransScript One-Step gDNA Removal and cDNA Synthesis SuperMix kit (AT311, TransGen Biotech, Beijing, China) and amplified in real-time quantitative PCR by a TransStart Top Green qPCR SuperMix kit (AQ131, TransGen Biotech). The following primer sequences were used: *Ptgs2*, 5'-CCACTTCAAGGGAGTCTGGA-3' (Forward), *Ptgs2*, 5'-AGTCATCTGCTACGGGAGGA-3' (Reverse); *Gapdh*, 5'-AACTTTGGCATTGTGGAAGG-3' (Forward), *Gapdh*, 5'-GGATGCAGGGATGATGTTCT-3' (Reverse). Using the comparative threshold cycle (Ct), relative expression was calculated using $2^{-\triangle\triangle Ct}$ method and normalized by the expressions of *Gapdh* from the same samples.

Determination of glutathione (GSH) and malondialdehyde (MDA)

The cells and tumor tissues were lysed using RIPA lysis buffer containing 1 mM PMSF on ice for 30 min and then centrifuged at 12,000 × *g* at 4 °C for 10 min. Then, the resulting cell lysates were utilized to assess GSH content and MDA content, using commercially test kits (GSH, A061-1-1, Nanjing Jiancheng BioTechnology, Nanjing, China; MDA, S0131, Beyotime), respectively, according to the manufacturer's protocols.

Molecular docking

The molecular docking method was used for the analysis of indirubin and indigo binding with GSK-3β. The discovery Studio 3.0 docking program was adopted [25]. The structure of GSK-3β was downloaded

from PDB database (PDB ID: 2O5K). The preparation of protein structure included adding hydrogen atoms, removing water molecules, and assigning Charmm forcefield. All parameters were set as default.

Statistical analysis

Statistical analysis was performed using GraphPad Prism 6.0 software (San Diego, CA, USA). The statistical significance of differences between two groups was determined with unpaired Student's *t*-test and multiple comparisons were analyzed with one-way ANOVA. All data presented as mean ± standard deviation. Differences were considered statistically significant at $p < 0.05$.

Results

Low expression of Ptgs2 in breast cancer

There were 587, 343 and 564 DEGs between breast tumors and normal breast tissues from GSE20713, GSE154002 and GSE42568, respectively, *via* GEO2R online tools. Then, we used Venn diagram software to identify the commonly down-regulated genes in the three datasets. Results showed that a total of 16 down-regulated genes (log FC < -2, $P < 0.05$) was identified in the breast cancer tissues (Fig. 1A, B). Noticeably, *Ptgs2*, a ferroptosis marker, was down-regulated in breast cancer patients, which indicated that ferroptosis may be related to breast cancer [26, 27]. Furthermore, the prognostic information of *Ptgs2* was analyzed employing the Kaplan-Meier plotter. Result showed that the low mRNA expression of *Ptgs2* (HR, 0.82; CI, 0.7-0.96) was associated with the poorer overall survival for patients with breast cancer (Fig. 1C). In addition, we also performed GEPIA and found that *Ptgs2* mRNA was significantly lower in breast cancer tissues than that in normal tissues ($p < 0.05$) (Fig. 1D). Results above showed the low expression of *Ptgs2* in breast cancer.

Indirubin induces ferroptosis of breast cancer cell in vitro

In order to investigate whether indirubin has the inhibitory effect on breast cancer, we firstly performed wound healing assay to study the effect of indirubin on growth of 4T1 cells *in vitro*. As shown in Fig. 2A **and B**, indirubin (40 μM and 80 μM) significantly inhibited wound closure of 4T1 cells ($p < 0.05$, $p < 0.01$). Next, we detected the effect of indirubin on viability of 4T1 cells by MTT assay. Result showed that the viability of 4T1 cells was significantly inhibited in a dose-dependent manner after incubation with indirubin (Fig. 2C). These results demonstrated the anti-breast cancer effect of indirubin *in vitro*. Then, we explored whether ferroptosis was involved in the anti-breast cancer effect of indirubin. The pre-treatment of Fer-1 (ferrostatin-1, ferroptosis-specific inhibitor, 25 μM) significantly reversed indirubin-induced inhibition of 4T1 cells viability ($p < 0.05$) (Fig. 2D). However, Nec-1 (necrosis inhibitor, 50 μM) and z-VAD (apoptosis inhibitor, 50 μM) didn't protect 4T1 cells from indirubin-induced inhibition of viability (Fig. 2D). These results indicated indirubin induced ferroptosis of breast cancer cell *in vitro*. The occurrence of ferroptosis is characterized by the depletion of GSH and accumulation of lipid peroxides. Meanwhile, the result showed that indirubin (40 μM and 80 μM) reduced the GSH content of 4T1 cells ($p < 0.05$, $p < 0.05$) (Fig. 2E). MDA and 4-hydroxynonenal (4-HNE) are major end products derived from lipid peroxides. As

shown in Fig. 2F **and G**, indirubin (80 μM) significantly increased the level of MDA ($p < 0.05$) and 4-HNE ($p < 0.05$). In addition, glutathione peroxidase 4 (GPX4) plays a key role in reducing lipid peroxides. The expression level of GPX4 significantly decreased by indirubin (40 μM and 80 μM) ($p < 0.05$, $p < 0.05$) (Fig. 2G). These results indicated that indirubin induced ferroptosis of breast cancer cell *in vitro*.

Indirubin up-regulates the expression of PTGS2 in breast cancer cell

Given that low expression of *Ptgs2* in breast cancer found by bioinformatics analysis in Fig. 1, We sought to explore whether indirubin-induced ferroptosis was related to PTGS2. We firstly detected the effects of indirubin on the expression of PTGS2 by qPCR and Western blotting. As shown in Fig. 3A, indirubin (40 μM and 80 μM) significantly elevated the mRNA level of *Ptgs2* in 4T1 cells ($p < 0.01$, $p < 0.001$). Moreover, indirubin (80 μM) significantly increased the expression level of PTGS2 protein ($p < 0.05$) (Fig. 3B). Indirubin was reported as the potent inhibitor of glycogen synthase kinase-3 beta (GSK-3β) [28]. We found that indirubin could form hydrogen bonds with Arg141, Gln185 and Val135 of GSK-3β protein by molecular docking (Fig. 3C, D). Interestingly, indigo, a main component from *Indigo Naturalis* and isomer of indirubin, only forms the hydrogen bond with Arg141of GSK-3β (Fig. 3C, D). It was indicated that two carbonyl groups in opposite positions of indirubin benefited its binding with GSK-3β. We further analyzed the effect of indirubin on phosphorylation (Ser 9) of GSK-3β in 4T1 cells by western blotting. Indirubin but indigo could promote phosphorylation (Ser 9) of GSK-3β (Fig. 3E). Correspondingly, indigo had no effect on the mRNA and protein expression of PTGS2 (Fig. 3F, G). In addition, indigo failed to triggering lipid peroxidation and ferroptosis (Fig. 3H **and Supplementary Fig. 1**). Indeed, it has been reported that GSK-3β participates in regulating the expression of PTGS2 [29, 30]. Hence, we speculated that indirubin may regulate the activity of GSK-3β to promote the expression of PTGS2 and then trigger the ferroptosis of tumor cells.

Indirubin suppresses breast cancer in vivo

Indirubin has been shown *in vitro* to induce ferroptosis of breast cancer cells, which may concern up-regulation of *Ptgs2*. Therefore, we next sought to investigate whether indirubin could suppress breast cancer *in vivo*. Firstly, we evaluated the anti-tumor activity of indirubin using the mouse model of breast cancer by injection of 4T1 cells subcutaneously. Results showed that indirubin (20 mg/kg) significantly inhibited the growth of breast cancer with reduced tumor weight ($p < 0.05$) and volume ($p < 0.01$) compared with the control group (Fig. 4A-C). Histopathological observation of tumor tissue showed that indirubin resulted in breast tumor necrosis (Fig. 4D). Meanwhile, the positive drug ADR suppressed breast cancer (Fig. 4A-D). After indirubin (20 mg/kg) treatment, the GSH content of tumor tissues significantly decreased ($p < 0.05$) (Fig. 4F). Indirubin (10 mg/kg and 20 mg/kg) significantly increased the MDA level of tumor tissues ($p < 0.01$, $p < 0.01$) (Fig. 4G). In addition, indirubin also increased the 4-HNE level of tumor tissues, and decreased the expression of GPX4 of tumor tissues (Fig. 4E). As expected, Indirubin (10 mg/kg and 20 mg/kg) significantly increased the level of PTGS2 protein of tumor tissues ($p < 0.01$, p

< 0.001) (Fig. 4H). However, treatment of indigo (20 mg/kg) didn't decrease the weight and volume of breast tumors and promote necrosis and lipid peroxidation of tumors consistent with *in vitro* results (Fig. 4). The results showed that indirubin promoted lipid peroxidation of tumors suppressed breast cancer in *vivo*.

Discussion

Breast cancer is one of the leading causes of cancer death in women. Chemotherapy is one of the effective but risky ways to treat breast cancer. Naturally derived compounds have the potential to develop new drugs because of their safety and efficacy. Indirubin and derivatives has the inhibitory effect on tumors [15–17]. In our study, effectiveness and pharmacological mechanism of indirubin was explored, which may contribute to development of anti-breast cancer drug.

Ferroptosis is a unique way of cell death, and it has been shown that ferroptosis plays an important role in the occurrence and development of tumors [31]. By inducing ferroptosis of tumor cells, it can be used for tumor therapy [32, 33]. *Ptgs2*, also known as cyclooxygenase-2 (Cox-2), is the key enzyme in prostaglandin biosynthesis. As a matter of fact, cyclooxygenases can catalyze lipid oxidation [34, 35]. Studies have shown that *Ptgs2* is involved in the process of ferroptosis, and *Ptgs2* is significantly up-regulated in the ferroptosis induced by RSL3 and erastin [36]. Meanwhile, suppression of *Ptgs2* can inhibit the ferroptosis of cells and play a protective role [26, 27]. In our study, results of bioinformatical analysis showed that ferroptosis-related gene *Ptgs2* was expressed lower in breast cancer, which indicated an efficient strategy for treating breast cancer. It is possible to induce ferroptosis of breast cancer cells by ug-regulation of *Ptgs2*. Then, *in vivo* and *in vitro* analysis results showed that indirubin could play an anti-breast cancer role by upregulation of *Ptgs2* to induce ferroptosis.

GSK-3β is a protein related to the regulation of *Ptgs2*, which can increase the expression of *Ptgs2* by inhibiting GSK-3β activity [30]. The activity of GSK-3β is regulated by phosphorylation at Ser 9 and Tyr 216 in opposing directions, with phosphorylation of Ser 9 decreasing GSK-3β activity and phosphorylation of Tyr 216 increasing GSK-3β activity [37]. However, previous studies have shown that indirubin is an inhibitor of GSK-3β [28]. Our results showed that indirubin promoted phosphorylation of GSK-3β at Ser 9 and then inhibited the activity of GSK-3β. Molecular docking further proved that indirubin with two carbonyl groups at different sides could form additional hydrogen bonds with Gln185 and Val135 of GSK-3β, compared to indigo with two carbonyl groups the same side indicating the special role of indirubin in regulating GSK-3β.

Conclusion

In conclusion, indirubin suppresses breast cancer by up-regulation of Ptgs2 and induction of ferroptosis in vitro and in vivo in a 4T1 murine breast cancer model, which may be related bind of indirubin with GSK-3β and then promote its phosphorylation at Ser 9 (**Fig. 5**).

Declarations

Acknowledgements

Not applicable.

Authors' Contributions

X.P. Kuang performed the experiments, acquired and analyzed all the data. Y.N. Jiang and J.W. Huang drafted the manuscript. W.X. Li and Y.Z. Guo designed the research, revised and approved the manuscript. All authors read and approved final manuscript.

Funding

This work was supported by the Yunnan Provincial Science and Technology Department-Applied Basic Research Joint Special Funds of Yunnan University of Chinese Medicine (2019FF002 (-007), 2017FF116 (-015)); National Natural Science Foundation of China (81560661, 81960780). They had no role in the design of the study; collection, analysis, and interpretation of the data; or writing of the manuscript.

Availability of data and materials

The datasets used and/or analyzed during the current study are available from the corresponding author on reasonable request.

Ethics approval and consent to participate

Animal experiments were approved by the Animal Care and Use Committee of Jinan University and conducted in accordance with National Institute of Health's Guide for the Care and Use of Laboratory Animals (7th edition, United States).

Consent for publication

Not applicable.

Competing interests

The authors declare that they have no competing interests.

Abbreviations

4-HNE, 4-hydroxynonenal; Cox-2, cyclooxygenase-2; CML, chronic myelocytic leukemia; DEGs, differentially expressed genes; DMSO, dimethyl sulfoxide; FBS, fetal bovine serum; GPX4, glutathione peroxidase 4; GSH, glutathione; GSK-3β, Glycogen synthase kinase 3β; H&E, hematoxylin and eosin; MDA, malondialdehyde; MTT, 3-(4,5-dimethyl-2-thiazolyl)-2,5-diphenyl-2-H-tetrazolium bromide; PBS, phosphate buffer saline; *Ptgs2, prostaglandin-endoperoxide synthase 2.*

References

1. Porter PL: Global trends in breast cancer incidence and mortality. *Salud Publica Mex* 2009, 51:s141-s146. https://doi.org/10.1590/s0036-36342009000800003
2. DeSantis CE, Bray F, Ferlay J, Lortet-Tieulent J, Anderson BO, Jemal A: International variation in female breast cancer incidence and mortality rates. *Cancer Epidemiol Biomarkers Prev* 2015, 24(10):1495-1506. https://doi.org/10.1158/1055-9965.epi-15-0535
3. Ghoncheh M, Pournamdar Z, Salehiniya H: Incidence and mortality and epidemiology of breast cancer in the world. *Asian Pac J Cancer Prev* 2016, 17(S3):43-46. https://doi.org/10.7314/apjcp.2016.17.s3.43
4. Marquette C, Nabell L: Chemotherapy-resistant metastatic breast cancer. *Curr Treat Options Oncol* 2012, 13(2):263-275. https://doi.org/10.1007/s11864-012-0184-6
5. Naito Y, Kai Y, Ishikawa T, Fujita T, Uehara K, Doihara H, Tokunaga S, Shimokawa M, Ito Y, Saeki T: Chemotherapy-induced nausea and vomiting in patients with breast cancer: a prospective cohort study. *Breast Cancer* 2020, 27(1):122-128. https://doi.org/10.1007/s12282-019-01001-1
6. Partridge AH, Burstein HJ, Winer EP: Side effects of chemotherapy and combined chemohormonal therapy in women with early-stage breast cancer. *J Natl Cancer Inst Monogr* 2001, 2001(30):135-142. https://doi.org/10.1093/oxfordjournals.jncimonographs.a003451
7. Kawai S, Iijima H, Shinzaki S, Hiyama S, Yamaguchi T, Araki M, Iwatani S, Shiraishi E, Mukai A, Inoue T: Indigo Naturalis ameliorates murine dextran sodium sulfate-induced colitis via aryl hydrocarbon receptor activation. *J Gastroenterol* 2017, 52(8):904-919. https://doi.org/10.1007/s00535-016-1292-z
8. Zhang T, Huang H-z, Xu R-c, Wang J-b, Yang M, Cao J-h, Zhang Y, Zhang D-k, Han L: An anti-influenza virus activity-calibrated chemical standardization approach for quality evaluation of indigo naturalis. *Anal Methods* 2019, 11(37):4719-4726.
9. Chiang Y-R, Li A, Leu Y-L, Fang J-Y, Lin Y-K: An in vitro study of the antimicrobial effects of indigo naturalis prepared from Strobilanthes formosanus Moore. *Molecules* 2013, 18(11):14381-14396. https://doi.org/10.3390/molecules181114381
10. Wang L, Zhou G-B, Liu P, Song J-H, Liang Y, Yan X-J, Xu F, Wang B-S, Mao J-H, Shen Z-X: Dissection of mechanisms of Chinese medicinal formula Realgar-Indigo naturalis as an effective treatment for

promyelocytic leukemia. *Proc Natl Acad Sci USA* 2008, 105(12):4826-4831. https://doi.org/10.1073/pnas.0712365105

11. Cheng H-M, Wu Y-C, Wang Q, Song M, Wu J, Chen D, Li K, Wadman E, Kao S-T, Li T-C: Clinical efficacy and IL-17 targeting mechanism of Indigo naturalis as a topical agent in moderate psoriasis. *BMC Complement Altern Med* 2017, 17(1):1-11. https://doi.org/10.1186/s12906-017-1947-1
12. Gaboriaud-Kolar N, Vougogiannopoulou K, Skaltsounis A-L: Indirubin derivatives: A patent review (2010–present). *Expert Opin Ther Pat* 2015, 25(5):583-593. https://doi.org/10.1517/13543776.2015.1019865
13. Hoessel R, Leclerc S, Endicott JA, Nobel ME, Lawrie A, Tunnah P, Leost M, Damiens E, Marie D, Marko D: Indirubin, the active constituent of a Chinese antileukaemia medicine, inhibits cyclin-dependent kinases. *Nat Cell Biol* 1999, 1(1):60-67. https://doi.org/10.1038/9035
14. Xiao Z, Hao Y, Liu B, Qian L: Indirubin and meisoindigo in the treatment of chronic myelogenous leukemia in China. *Leuk Lymphoma* 2002, 43(9):1763-1768. https://doi.org/10.1080/1042819021000006295
15. Aobchey P, Sinchaikul S, Phutrakul S, Chen S-T: Simple purification of indirubin from Indigofera tinctoria Linn. and inhibitory effect on MCF-7 human breast cancer cells. *Chiang Mai J Sci* 2007, 34:329-337.
16. Braig S, Kressirer CA, Liebl J, Bischoff F, Zahler S, Meijer L, Vollmar AM: Indirubin derivative 6BIO suppresses metastasis. *Cancer Res* 2013, 73(19):6004-6012. https://doi.org/10.1158/0008-5472.can-12-4358
17. Nam S, Buettner R, Turkson J, Kim D, Cheng JQ, Muehlbeyer S, Hippe F, Vatter S, Merz K-H, Eisenbrand G: Indirubin derivatives inhibit Stat3 signaling and induce apoptosis in human cancer cells. *Proc Natl Acad Sci USA* 2005, 102(17):5998-6003. https://doi.org/10.1073/pnas.0409467102
18. Eling N, Reuter L, Hazin J, Hamacher-Brady A, Brady NR: Identification of artesunate as a specific activator of ferroptosis in pancreatic cancer cells. *Oncoscience* 2015, 2(5):517. https://doi.org/10.18632/oncoscience.160
19. Louandre C, Ezzoukhry Z, Godin C, Barbare JC, Mazière JC, Chauffert B, Galmiche A: Iron-dependent cell death of hepatocellular carcinoma cells exposed to sorafenib. *Int J Cancer* 2013, 133(7):1732-1742. https://doi.org/10.1002/ijc.28159
20. Ma S, Dielschneider RF, Henson ES, Xiao W, Choquette TR, Blankstein AR, Chen Y, Gibson SB: Ferroptosis and autophagy induced cell death occur independently after siramesine and lapatinib treatment in breast cancer cells. *PLoS One* 2017, 12(8):e0182921. https://doi.org/10.1371/journal.pone.0182921
21. Chen G-Q, Benthani FA, Wu J, Liang D, Bian Z-X, Jiang X: Artemisinin compounds sensitize cancer cells to ferroptosis by regulating iron homeostasis. *Cell Death Differ* 2020, 27(1):242-254. https://doi.org/10.1038/s41418-019-0352-3
22. Davis S, Meltzer PS: GEOquery: a bridge between the Gene Expression Omnibus (GEO) and BioConductor. *Bioinformatics* 2007, 23(14):1846-1847.

https://doi.org/10.1093/bioinformatics/btm254

23. Hou G-X, Liu P, Yang J, Wen S: Mining expression and prognosis of topoisomerase isoforms in non-small-cell lung cancer by using Oncomine and Kaplan–Meier plotter. *PloS One* 2017, 12(3):e0174515. https://doi.org/10.1371/journal.pone.0174515
24. Tang Z, Li C, Kang B, Gao G, Li C, Zhang Z: GEPIA: a web server for cancer and normal gene expression profiling and interactive analyses. *Nucleic Acids Res* 2017, 45(W1):W98-W102. https://doi.org/10.1093/nar/gkx247
25. Wu G, Robertson DH, Brooks III CL, Vieth M: Detailed analysis of grid-based molecular docking: A case study of CDOCKER—A CHARMm-based MD docking algorithm. *J Comput Chem* 2003, 24(13):1549-1562. https://doi.org/10.1002/jcc.10306
26. Li Q, Han X, Lan X, Gao Y, Wan J, Durham F, Cheng T, Yang J, Wang Z, Jiang C: Inhibition of neuronal ferroptosis protects hemorrhagic brain. *JCI Insight* 2017, 2(7). https://doi.org/10.1172/jci.insight.90777
27. Xiao X, Jiang Y, Liang W, Wang Y, Cao S, Yan H, Gao L, Zhang L: miR-212-5p attenuates ferroptotic neuronal death after traumatic brain injury by targeting Ptgs2. *Mol Brain* 2019, 12(1):78. https://doi.org/10.1186/s13041-019-0501-0
28. Leclerc S, Garnier M, Hoessel R, Marko D, Bibb JA, Snyder GL, Greengard P, Biernat J, Wu Y-Z, Mandelkow E-M: Indirubins Inhibit Glycogen Synthase Kinase-3β and CDK5/P25, Two Protein Kinases Involved in Abnormal Tau Phosphorylation in Alzheimer's Disease A PROPERTY COMMON TO MOST CYCLIN-DEPENDENT KINASE INHIBITORS? *J Biol Chem* 2001, 276(1):251-260. https://doi.org/10.1074/jbc.m002466200
29. Ye Z, Wang N, Xia P, Wang E, Yuan Y, Guo Q: Delayed administration of parecoxib, a specific COX-2 inhibitor, attenuated postischemic neuronal apoptosis by phosphorylation Akt and GSK-3β. *Neurochem Res* 2012, 37(2):321-329. https://doi.org/10.1007/s11064-011-0615-y
30. Bai L, Chang H-M, Cheng J-C, Chu G, Leung PC, Yang G: Lithium Chloride Increases COX-2 Expression and PGE2 Production in a Human Granulosa-Lutein SVOG Cell Line Via a GSK-3 β/β-Catenin Signaling Pathway. *Endocrinology* 2017, 158(9):2813-2825. https://doi.org/10.1210/en.2017-00287
31. Lu B, Chen XB, Ying MD, He QJ, Cao J, Yang B: The role of ferroptosis in cancer development and treatment response. *Front Pharmacol* 2018, 8:992. https://doi.org/10.3389/fphar.2017.00992
32. Shen Z, Song J, Yung BC, Zhou Z, Wu A, Chen X: Emerging strategies of cancer therapy based on ferroptosis. *Adv Mater* 2018, 30(12):1704007. https://doi.org/10.1002/adma.201704007
33. Lachaier E, Louandre C, Godin C, Saidak Z, Baert M, Diouf M, Chauffert B, Galmiche A: Sorafenib induces ferroptosis in human cancer cell lines originating from different solid tumors. *Anticancer Res* 2014, 34(11):6417-6422.
34. Liu X, Moon SH, Jenkins CM, Sims HF, Gross RW: Cyclooxygenase-2 mediated oxidation of 2-arachidonoyl-lysophospholipids identifies unknown lipid signaling pathways. *Cell Chem Biol* 2016, 23(10):1217-1227. https://doi.org/10.1016/j.chembiol.2016.08.009

35. Bretscher P, Egger J, Shamshiev A, Trötzmüller M, Köfeler H, Carreira EM, Kopf M, Freigang S: Phospholipid oxidation generates potent anti-inflammatory lipid mediators that mimic structurally related pro-resolving eicosanoids by activating Nrf2. *EMBO Mol Med* 2015, 7(5):593-607. https://doi.org/10.15252/emmm.201404702

36. Yang WS, SriRamaratnam R, Welsch ME, Shimada K, Skouta R, Viswanathan VS, Cheah JH, Clemons PA, Shamji AF, Clish CB: Regulation of ferroptotic cancer cell death by GPX4. *Cell* 2014, 156(1-2):317-331. https://doi.org/10.1016/j.cell.2013.12.010

37. Forde Ja, Dale TC: Glycogen synthase kinase 3: a key regulator of cellular fate. *Cell Mol Life Sci* 2007, 64(15):1930-1944. https://doi.org/10.1007/s00018-007-7045-7

Figures

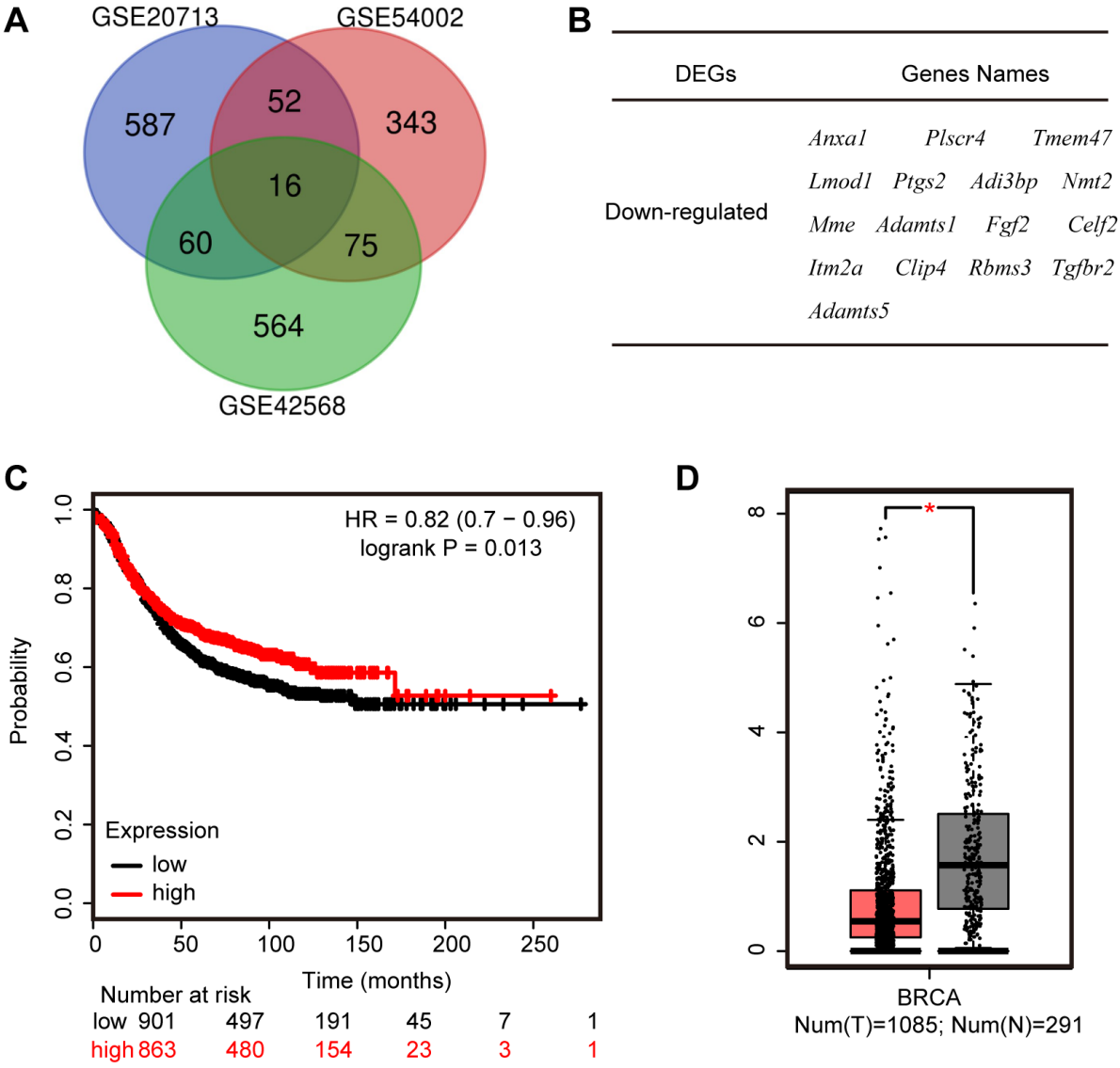

Figure 1

Low Expression of Ptgs2 in Breast Cancer. (A and B) Authentication of 16 down-regulated genes (log FC < -2) in breast tumor compared to normal breast tissues from the three datasets (GSE20713, GSE54002 and GSE42568) by Venn diagrams. (C) The prognostic information of Ptgs2 was showed by Kaplan-Meier plotter. (D) Gene Expression Profiling Interaction Analysis (GEPIA) for the expression of Ptgs2 in tumor tissues (red box) and normal tissues (gray box). T, tumor tissues; N, normal tissues. *p < 0.05 vs. normal tissues.

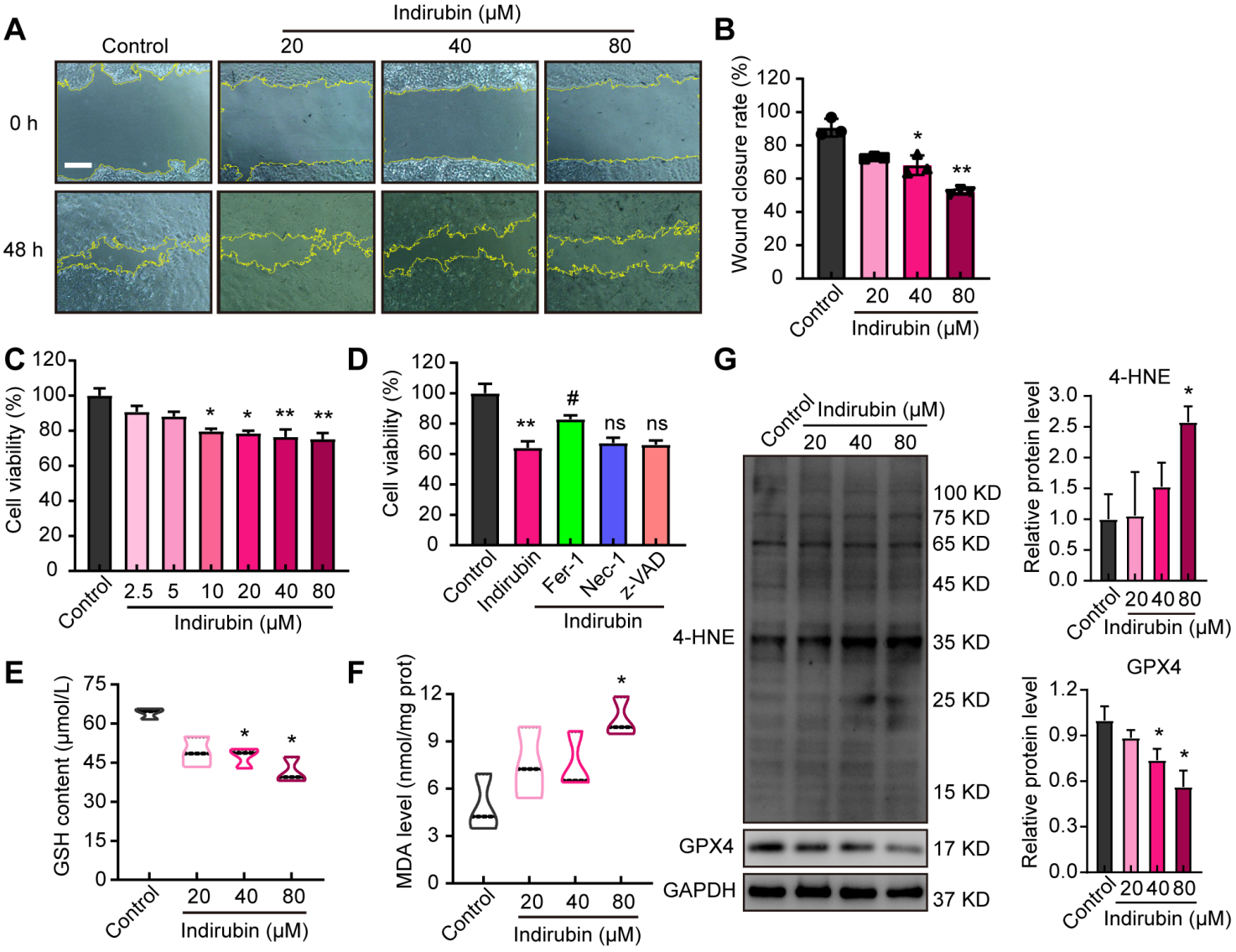

Figure 2

Indirubin induces ferroptosis of breast cancer cell in vitro. (A-B) Representative images of cell migration and quantitative analysis of wound closure rate. Scale bar: 200 μm. (C) The viability of 4T1 cells with indirubin at indicated concentrations for 24 h. (D) The viability of 4T1 cells pretreated with Fer-1 (25 μM), Nec-1 (50 μM) or z-VAD (50 μM) and then with indirubin (80 μM). (E) The GSH content of 4T1 cells. (F) The MDA level of 4T1 cells. (G) Western blotting detection for 4-HNE and GPX4 and quantitative analysis. *p < 0.05, **p < 0.01 and ***p < 0.001 vs. Control group; ns (not significant), #p < 0.05 vs. Indirubin group.

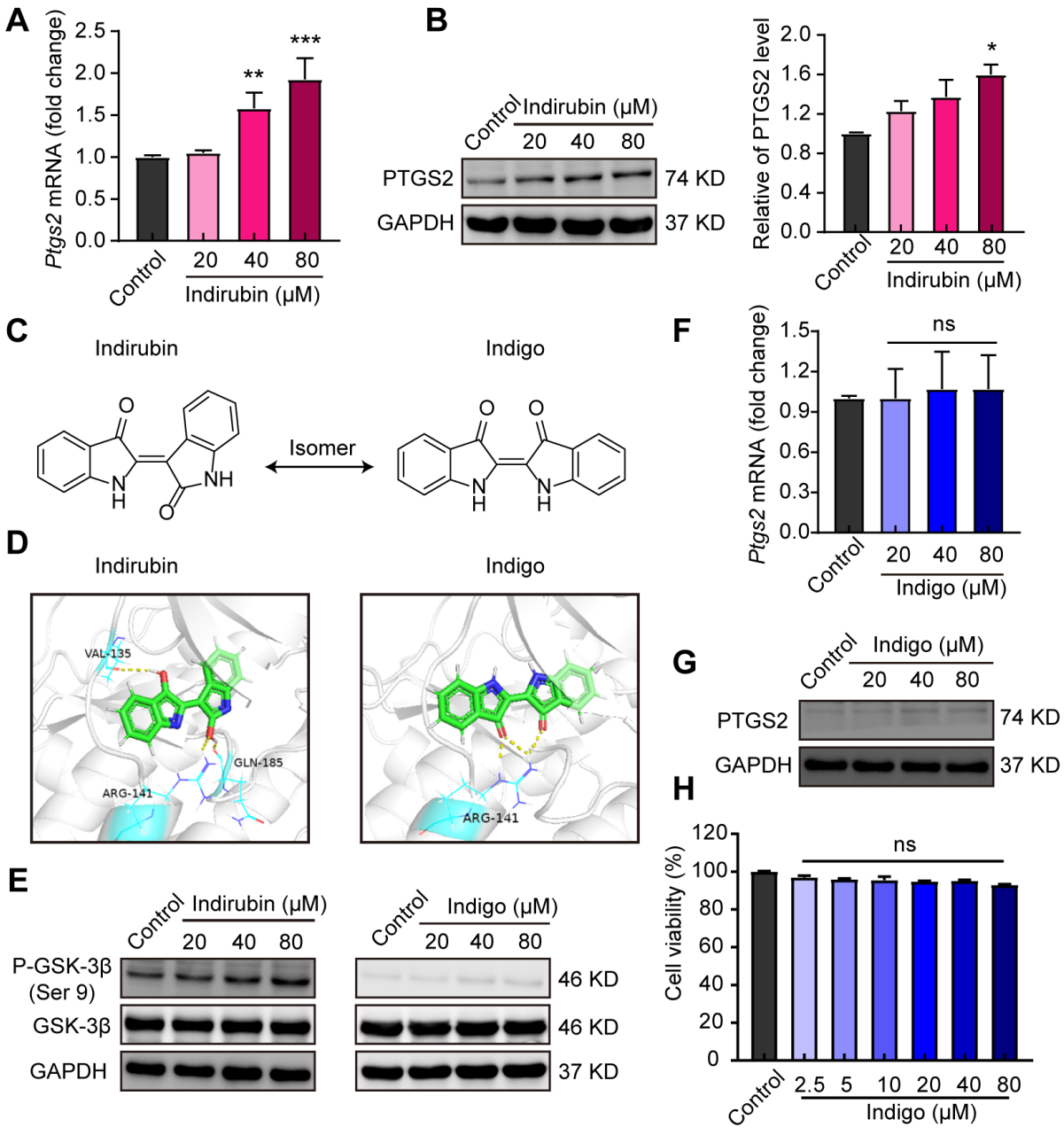

Figure 3

Indirubin up-regulates the expression of PTGS2 in breast cancer cell. (A) The mRNA level of Ptgs2 in 4T1 cells with indirubin. (B) Western blotting for PTGS2 in 4T1 cells with indirubin and quantitative analysis. (C) Chemical structure of indirubin and indigo. (D) Molecular docking of indirubin and indigo with GSK-3β. Yellow dot line indicated interaction of hydrogen bond. (E). Western blotting for P-GSK-3β (Ser 9) and GSK-3β in 4T1 cells with indirubin or indigo. (F) The mRNA level of Ptgs2 in 4T1 cells with indigo. (G) Western blotting for PTGS2 in 4T1 cells with indigo. (H) The viability of 4T1 cells with indigo at indicated concentrations for 24 h. ns (not significant), *p < 0.05, **p < 0.01 and ***p < 0.001 vs. Control group.

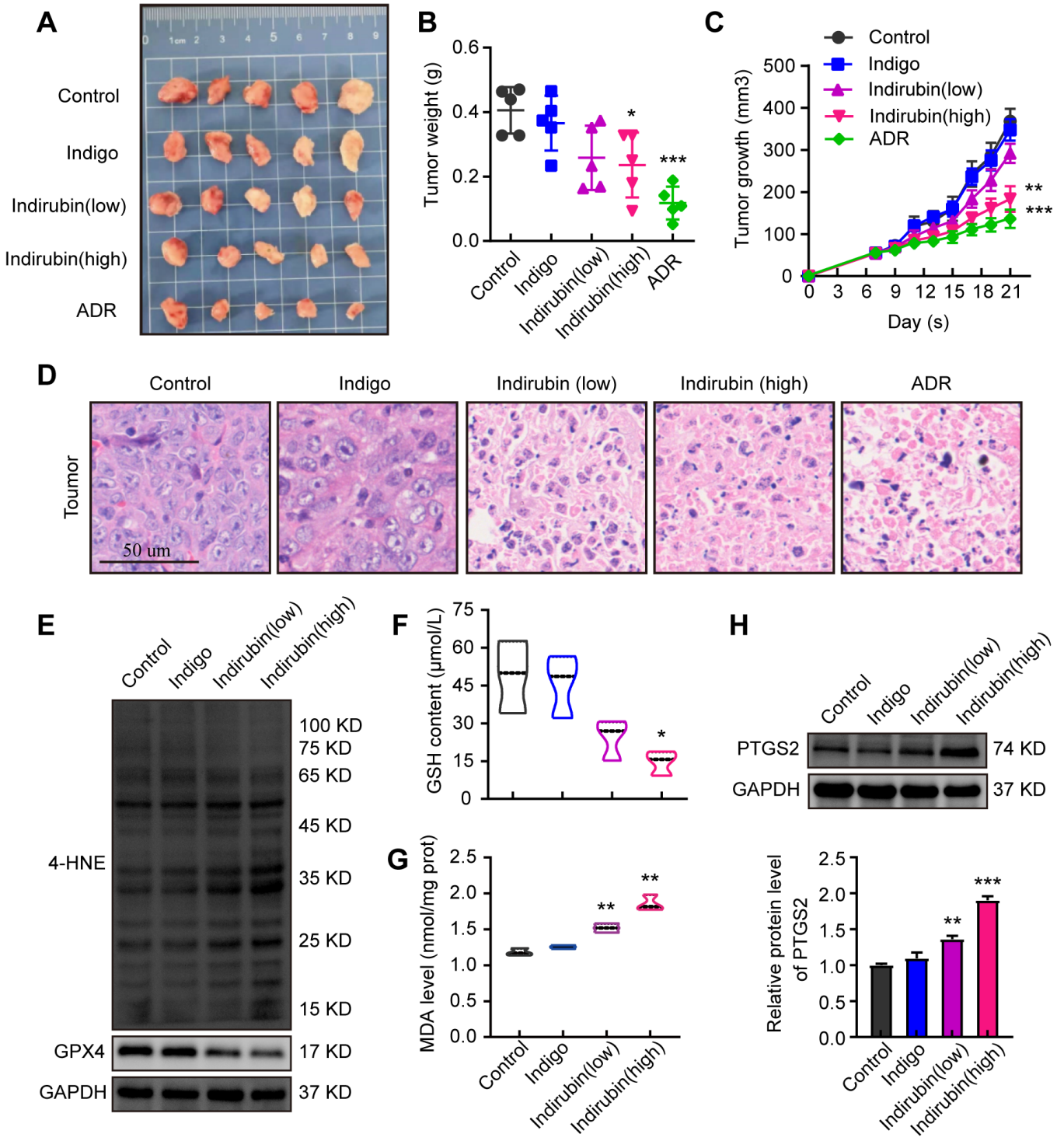

Figure 4

Indirubin suppresses breast cancer in vivo. (A) The picture of tumors in different groups of mice (n=5). (B) Tumor volume of mice in each group was determined at the end of treatment (n=5). (C) Tumor growth curves of different groups of mice (n=5). (D) Histological images of tumors sections stained by H&E. Scale bar: 50 μm. (E) Western blotting detection for 4-HNE and GPX4. (F) The GSH content of tumor tissues. (G) The MDA level in tumor tissues. (H) Western blotting for PTGS2 protein and quantitative analysis. *p < 0.05, **p < 0.01 and ***p < 0.001 vs. Control group.

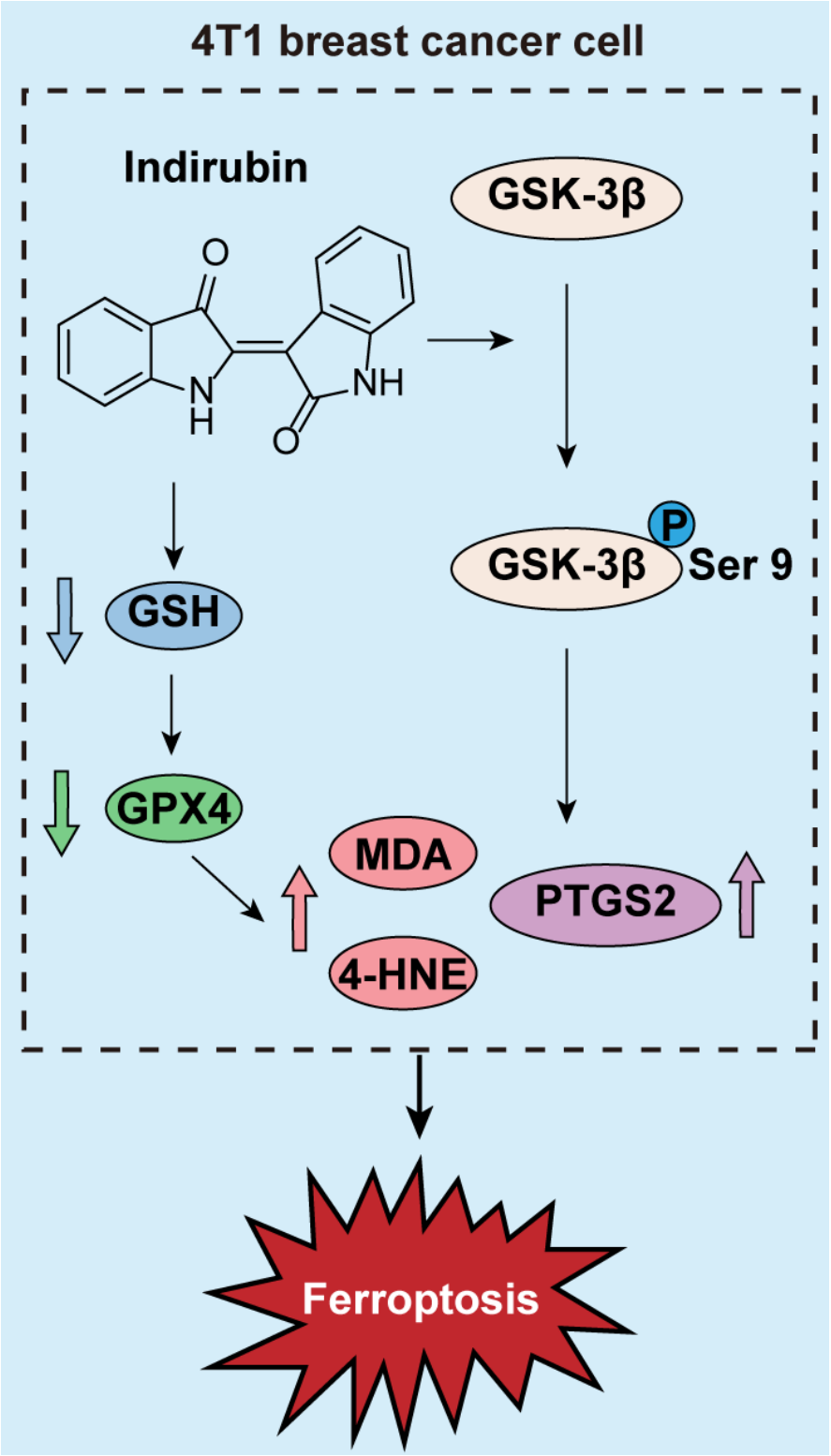

Figure 5

The mechanism diagram of indirubin against 4T1 breast cancer model in vitro and in vivo.

Supplementary Files

This is a list of supplementary files associated with this preprint. Click to download.

- Additionalfile1SupplementaryFigure101.tif
- Additionalfile2SupplementaryFigure201.tif
- Additionalfile3SupplementaryFigure301.tif
- Additionalfile4SupplementaryFigure401.tif
- Additionalfile5SupplementaryFigure501.tif
- Additionalfile6SupplementaryTable1.docx
- Additionalfile7TheARRIVEchecklist.docx